A FRESH LOOK AT PARTICLE SIZE DISTRIBUTIONS AND THE PERFORMANCE

CHARACTERISTICS OF AMBIENT PARTICULATE MATTER SAMPLERS

Brent W. Auvermann[1], Calvin B. Parnell, Jr.[2], Bryan W. Shaw[3] and Arturo Romanillos[4]

Abstract

A thorough understanding of (a) the technical aspects of measuring airborne particulate matter (PM) and (b) how to interpret those measurements in light of health-based ambient standards is central to ensuring that air quality regulations achieve their objectives with regard to human exposure to PM. This paper takes a fresh look at the mathematics and engineering of sampler performance in order to specify the circumstances under which it is appropriate to infer fine-particle concentrations from particle-size distributions of coarser PM fractions sampled with non-ideal samplers. We adopt a notation that corresponds to the mathematical language of statistics and variable transformation. We assume at least a working knowledge of air sampling techniques, particle size distributions, probability theory and integral calculus.

Variable Definitions

The variables in this paper are defined as follows, with units given in brackets [ ]:

δ Aerodynamic equivalent diameter (AED) of a suspended particle [μm]

$p(\delta)$ Differential probability that random particles within a sample will have an AED arbitrarily close to the value δ [μm^{-1}]

$P(\delta)$ Cumulative probability that random particles within a sample will have an AED arbitrarily close to the value δ [ ]

C Mass of PM contained in a reference volume of air [μg]

$m(\delta)$ Differential mass distribution of particles within a sample [μg μm^{-1}]

$M(\delta)$ Cumulative mass distribution of particles within a sample [μg]

$\varepsilon(\delta)$ Fractional penetration efficiency of a PM preseparator [ ]

d_m Mass-median diameter of a sample of PM [μm]

d_c Sampler cutpoint, or AED at which the fractional penetration efficiency is 50% [μm]

d_{max} Maximum AED of all particles suspended in ambient air [μm]

σ_g Geometric standard deviation [ ]

$i=x, y$ Subscripts denoting samplers with cutpoints $d_c=x$ and $d_c=y$, respectively

$j=a, s$ Subscripts denoting PM in the ambient (a) or sampled (s) air

Background and Theoretical Development

Particles suspended in air react to drag, gravitational and buoyant forces according to their density, shape, roughness, orientation and rotation (or spin). Their reaction to body forces is also related to the properties and dynamic characteristics of the air in which they are suspended. Because the aerodynamic properties of a suspended particle of arbitrary shape generally defy

[1]Assistant Professor of Agricultural Engineering, Texas A&M University System, 6500 Amarillo Blvd. West, Amarillo, TX 79106. [2]Regents Professor of Agricultural Engineering, Texas A&M University, 207 Scoates Hall, College Station, TX 77843-2117. [3]Associate Professor of Agricultural Engineering, Texas A&M University System, 303 Scoates Hall, College Station, TX 77843-2121. [4]Assistant Research Engineer (feedlot hydrology), Texas Agricultural Experiment Station, 6500 Amarillo Blvd. West, Amarillo, TX 79106.

derivation from first principles, those properties must be inferred using the classical, inverse problem of experimental dynamics: measure the performance of the particle in a range of conditions, then fit the resulting performance curves with empirically-derived parameters in a suitable aerodynamic model such as the Navier-Stokes equation (NS) or its appropriate simplified forms.

Complicating the matter further, ambient PM consists of a wide range of particle sizes, materials and shapes. Consequently, the empirically derived aerodynamic parameters must be measured for the ensemble of particles, representing some kind of average of the aerodynamic parameters of the individual particles. The manner in which the individual parameters are averaged (in the empirical sense) depends heavily on the experimental apparatus used and the fluid dynamics characteristic of the apparatus in its designed range of operation. For example, to the extent that particle orientation affects the aerodynamic performance of individual suspended particles, samplers whose design flow regimes preferentially impose certain orientations (i. e., with respect to the flow streamlines) upon suspended particles will give rise to unique ensemble averages of those parameters. Thus, empirically derived aerodynamic parameters are instrument-dependent.

The Mathematical Background of Aerosol Measurement

The ensemble average values of the aerodynamic parameters are also influenced by the statistical distribution of particle sizes in the ensemble. The *particle-size distribution* (PSD) of an ensemble of suspended particles (henceforth, an *aerosol*) may be expressed in several ways. The PSDs that are most relevant to current air-quality regulations and health-based standards are those that relate the aerodynamic performance of discrete subsets of an aerosol to the incremental mass of that subset in the air. For a sample of PM having a sufficiently large number of particles, the PSD approaches a continuum on the range of particle sizes represented by the sample. Mathematically, that relationship is expressed in the dimensionless *probability distribution* (or *frequency distribution*) p(δ), an example of which is graphically illustrated in Figure 1.

By definition, the area under the curve p(δ) is unity[5]:

$$\int_{-\infty}^{\infty} p(\delta)d\delta = 1 \qquad [1]$$

Because the function p(δ) is a dimensionless probability density function, we may multiply p(δ) by the total sample mass C_s to obtain a new function m(δ) having both dimension and physical meaning:

$$m(\delta) = C_s\, p(\delta) \qquad [2]$$

The function m(δ) represents the differential total mass of particles in the sample having an AED arbitrarily close to the value δ. In general, we may integrate m(δ) on any interval [$0 < x < \delta$] to obtain the cumulative mass distribution function, M(δ):

---

[5]For situations of practical interest, (a) aerodynamic particle diameter is strictly non-negative, and (b) ambient particles that remain suspended in air tend to have a maximum aerodynamic diameter, which we denote as d_{max}. In Equation [1], we have retained the full domain for the sake of complete statistical generality, but in subsequent developments, we have truncated the lower and upper bounds on δ at $\delta=0$ and $\delta=d_{max}$, respectively, with no loss in generality.

$$M(\delta) = C_s \int_{-\infty}^{\delta} p(x)dx = \int_{-\infty}^{\delta} m(x)dx \qquad [3]$$

The function $M(\delta)$ has an important interpretation for PM sampling; it represents the total mass of particles within the sample having an AED less than or equal to the value δ.

Finally, we may normalize the function $M(\delta)$ by dividing Equation [3] by the total mass of particles in the sample, C_s, to obtain the dimensionless cumulative distribution function, $P(\delta)$:

$$P(\delta) = \int_{-\infty}^{\delta} p(x)dx \qquad [4]$$

The function $P(\delta)$ increases monotonically and takes on values between zero and unity (inclusive). $P(\delta)$ may never be greater than unity. Physically, $P(\delta)$ represents the mass fraction of particles in the sample having an AED less than or equal to δ. For example, Figure 2 is a graph of $P_s(\delta)$ for a manufactured dust sample comprised of dried, ground and sieved feedyard manure.

The Mathematics of Sampler Performance

Having laid the mathematical foundation for understanding PSDs of airborne PM, we now turn our attention to engineering terms and the corresponding mathematical functions that help us to describe the performance of equipment designed to sample ambient PM. We first stipulate that, as a practical matter, no physical sampling device can possibly operate perfectly. Still, it is useful to consider the so-called *ideal* sampler in order to quantify the performance of actual samplers.

Ambient PM samplers approved for use in the federal regulatory framework are characterized by a preseparator, designed to collect the PM that is not relevant to the measurement, and a filter or membrane to collect the PM of interest. For example, the PM_{10} sampler consists of a vacuum pump that draws ambient air through a PM_{10} preseparator, which nominally collects the PM having an AED of 10μm or greater. The remaining particles remain entrained in the air and are collected on a special filter, which is then transported to a laboratory and weighed on a microbalance to determine the mass of PM deposited on the filter. That mass, determined by gravimetric difference, is considered the mass of PM_{10} in the sampled air.

We define the *ideal sampler* as a sampler that operates perfectly according to its purpose. For example, if we were interested in measuring the total amount of airborne PM between 2.5μm and 10μm AED, the ideal sampler for that purpose would preseparate from the sampled air every single particle having an AED outside the range 2.5-10μm, allowing all of the remaining particles to be captured in some measurement device. If we were interested in only those particles smaller than 2.5μm, the ideal sampler would preseparate from the sampled air every single particle larger than 2.5μm. Clearly, there is no single ideal sampler suitable for every task; the ideal sampler is defined by the purpose for which it is to be used.

In most regulatory applications, particularly those involving the National Ambient Air Quality Standards (NAAQS), the quantity of interest is the mass of particles having an AED less than or equal to a given value. For example, the NAAQS for the 24-hour average concentration of $PM_{2.5}$, 65 μg m^{-3}, refers to a concentration of all particles having an AED of 2.5μm or smaller. The ideal sampler in this case (USEPA, 1997b) is a sampler that (a) preseparates 100% of the particles having an AED greater than 2.5μm and (b) permits all of the particles having an AED of 2.5μm and smaller to be captured on a filter for subsequent gravimetric analysis. The same

concepts apply to the PM_{10} fraction; the ideal PM_{10} sampler preseparates all of the particles larger than AED=10μm and permits all of the remaining particles to be captured on a filter.

To illustrate the concept of the ideal PM_n sampler, where the dummy variable n is the size fraction [μm] of interest, we define the fractional penetration efficiency function, $\varepsilon(\delta)$, as follows:

$$\varepsilon(\delta) = \frac{C_{sp_s}(\delta)}{C_{ap_a}(\delta)} = \frac{m_s(\delta)}{m_a(\delta)} \qquad [5]$$

In Equation [5], the subscripts "a" and "s" refer to the *ambient* (actual) and *sampled* properties, respectively; that is, the efficiency $\varepsilon(\delta)$ describes the fraction of the *ambient* PM that penetrates through the preseparator and becomes part of the *sampled* PM. If $\varepsilon(\delta)=1.0$, then, the sampler is 100% efficient at permitting particles of AED=δ to penetrate through the sampler to the filter. Conversely, $\varepsilon(\delta)=0$ indicates that the preseparator collects all of the particles of AED=δ.

For the applications we are considering, the ideal PM_y sampler is characterized by the piecewise-continuous fractional penetration efficiency:

$$\varepsilon(\delta) \ = \ 1.0 \ \ [\delta <= y] \qquad [6]$$

$$\varepsilon(\delta) \ = \ 0.0 \ \ [\delta > y] \qquad [7]$$

The ideal PM_y sampler for y=10 (i. e., the ideal PM_{10} sampler) is represented by the graph of $\varepsilon(\delta)$ shown in Figure 3.

As noted above, actual samplers – no matter how well designed – cannot achieve the step singularity in the function $\varepsilon(\delta)$. Physically, the non-ideal nature of actual samplers shows up in two ways. First, the preseparator will always capture some small amount of the particles smaller than the design threshold. Second, the preseparator will always permit some particles larger than the design threshold to penetrate to the filter. Figure 4 shows how these inaccuracies are expressed in terms of the fractional penetration efficiency for an actual PM_{10} sampler.

The fractional penetration efficiency curve of a sampler is the basis for its classification as a Federal Reference Method (FRM) for monitoring PM (i. e., a sampler that may legally be used to determine compliance with the NAAQS). The shape and location of the function $\varepsilon(\delta)$ in relation to an idealized penetration efficiency curve (as shown in Figure 4) indicate how precisely the sampler approximates the ideal sampler. To elaborate on this point, we first define what we mean by a *PM_y sampler*, noting that this general discussion then applies equally well to PM_1, $PM_{2.5}$ or PM_{10} samplers (y=1, y=2.5 or y=10, respectively).

Let us consider a hypothetical, non-ideal sampler for which, using some reliable procedure, we have determined a fractional efficiency curve $\varepsilon(\delta)$. For the class of samplers needed for NAAQS compliance monitoring, $\varepsilon(\delta)$ is a monotonically decreasing sigmoid whose value approaches unity as δ vanishes and zero at some large particle size. Consequently, $\varepsilon(\delta)$ passes through a point (d_c, 0.5), which is known as the sampler's *cutpoint*. At this point, the sampler's fractional penetration efficiency is 50%. Further, $\varepsilon(\delta)$ passes through a point ($d_{0.84}$, 0.84). The value of the abscissa corresponds roughly to the particle diameter that lies one geometric standard deviation (i. e., one standard deviation of the log-transformed data) from the mean. The ratio

$$\sigma_g = d_c/d_{0.84} \qquad [8]$$

is an indicator of the "sharpness of cut," or the precision with which the preseparator approximates the ideal sampler's step discontinuity at the cutpoint. Ideal samplers (see Figure 4) have σ_g=1.0. Taken together, the two parameters d_c and σ_g represent performance specifications for an ambient sampler. Specifically, a sampler designed to monitor PM_y must have d_c=y (within some specified tolerance) and a σ_g approximately equal to the ideal value of 1.0 (again, within some specified tolerance).

In summary, as an example, the current Federal Reference Method (FRM) for PM_{10} sampling specifies three main criteria for designating a particular sampler as an FRM (USEPA, 1997a). First, the sampler must control the flow rate of air between 36 and 44 actual cubic feet per minute (acfm) for the duration of the sampling event. Second, the sampler must have a d_c between 9 and 11μm. Third, the characteristic slope of the fractional efficiency curve, σ_g, must be between 1.4 and 1.6. In general, those three considerations (flow rate, d_c and σ_g) represent performance-based criteria for FRM designation. Further, the FRM designation suggests that all samplers operating within those criteria will yield (a) equivalent results when operated side-by-side and therefore (b) comparable results when operated in different locations and conditions.

The latter inference, (b), is vitally important for monitoring networks because we must be confident that, when comparing air quality parameters at different locations, we are not "comparing apples to oranges." In other words, we must be confident that a Graseby FRM sampler operating in Denver, CO, a Wedding FRM sampler in Cleveland, OH, and a Rupprecht and Patashnick FRM sampler in Miami, FL are all measuring the same quantity. They will yield different results, but the numbers must be comparable. To ensure that the numbers are comparable, the samplers must be interchangeable.

A Critique of the Use of Coarse-Fraction PSDs to Infer Fine-Fraction Concentrations
Reliable and complete monitoring data on fine PM are hard to find and expensive to generate. In fact, as the PM fraction of interest gets smaller, the precision and cost of the sampling equipment and methods must necessarily increase. In the absence of such data, one obvious question that arises is, "can I infer fine PM concentrations from coarse PM observations?" A practical example is the attempt to infer $PM_{2.5}$ concentrations from a combination of PM_{10} measurements and subsequent PSD analysis of the exposed PM_{10} filters. In that case, the cost- and labor-saving objective would be to substitute an existing ambient monitor (PM_{10}) plus one additional step in the laboratory (PSD determination) for an additional, expensive and temperamental monitor such as the FRM $PM_{2.5}$ sampler.
The logic of this enterprise is straightforward. Consider again the hypothetical cumulative PSD shown in Figure 2. Assume for the sake of demonstration that this PSD was generated from a PM_{10} sampler. Further, let us assume that gravimetry yielded an ambient PM_{10} concentration of 100 μg m^{-3}. To estimate the $PM_{2.5}$ concentration, according to this method, we simply read from the cumulative PSD the % mass having AED<2.5μm, which in this case is 4%. Assuming, then, that 4% of the total sample mass was $PM_{2.5}$, we estimate that the $PM_{2.5}$ concentration was 0.04 x 100 μg m^{-3} = 4 μg m^{-3}.

Despite the straightforward appearance of that approach, it is fraught with subtle difficulties that may translate into significant errors. The most obvious is a practical difficulty: many compounds that form atmospheric $PM_{2.5}$ are volatile (potentially lost during gravimetric analysis of PM_{10} filters) or soluble (potentially lost in the electrolyte solutions used for optical determination of PSD). Because this difficulty is practical in nature, it is conceivable that changes in filter-handling protocol or selection of a more suitable suspension electrolyte could mitigate the errors that would otherwise result. In addition to that practical limitation, however, there is a more fundamental, theoretical limitation that we now explore.

To demonstrate this limitation, we first state the problem in mathematical terms. A coarse-particle sampler having a cutpoint at $d_c=y$ operates in PM-laden air characterized by an ambient mass loading C_a and an ambient, differential PSD represented by the function $p_a(\delta)$. The maximum particle AED in the ambient air is d_{max}. A collocated fine-particle sampler having a cutpoint at $d_c=x$ operates in the same ambient conditions. (The samplers will be designated PM_y and PM_x samplers, respectively, with $x<y$.) The fractional penetration efficiencies of the two samplers are $\varepsilon_y(\delta)$ and $\varepsilon_x(\delta)$, and the sample masses, using precise gravimetry, are C_{sy} and C_{sx}, respectively. Using some reliable means, the filter from the PM_y sampler has been subjected to a particle-size determination, and the cumulative sample PSD is represented by the function $P_{sy}(\delta)$. (Despite the additional conceptual difficulties implied by the distinction between physical/optical and aerodynamic particle size, we assume for the sake of argument that $P_{sy}(\delta)$ accurately reflects the distribution of *aerodynamic* diameters in the sample.)

In simple mathematical terms, the question is whether or not the product $C_{sy} P_{sy}(x)$ is an accurate approximation of, and therefore a substitute for, the "true" value C_{sx}. For a fixed value of y, the relative error of the approximation is a function of x and is given by $E(x)$ as follows:

$$E(x) = \frac{C_{sy} p_{sy}(x) - C_{sx}}{C_{sx}}$$ [9]

The function $E(x)$ may be rewritten in terms of the ambient PM loading and the performance characteristics of the samplers. First, we re-write Equation [5] for both the PM_y and PM_x samplers:

$$C_{sy} p_{sy}(\delta) = C_a p_a(\delta) \varepsilon_y(\delta)$$ [10]

$$C_{sx} p_{sx}(\delta) = C_a p_a(\delta) \varepsilon_x(\delta)$$ [11]

For a given value of y, we may integrate Equation [10] with respect to δ between the limits of $[0,x]$ to obtain:

$$C_{sy} \int_0^x p_{sy}(\delta) d\delta = C_a \int_0^x p_a(\delta) \varepsilon_y(\delta) d\delta$$ [12]

Similarly, we may integrate Equation [11] with respect to d between the limits of $[0,d_{max}]$:

$$C_{sx} \int_0^{d_{max}} p_{sx}(\delta) d\delta = C_a \int_0^{d_{max}} p_a(\delta) \varepsilon_x(\delta) d\delta$$ [13]

According to Equation [1] and inserting the physical upper and lower bounds $0<\delta<d_{max}$, the left-hand side of Equation [13] reduces to

$$C_{sx} = C_a \int_0^{d_{max}} p_a(\delta) \varepsilon_x(\delta) d\delta$$ [14]

The integral on the left-hand side of Equation [12] may be evaluated using Equation [4]:

$$C_{sy} P_{sy}(x) = C_a \int_0^x p_a(\delta) \varepsilon_y(\delta) d\delta$$ [15]

Substituting Equations [14] and [15] into Equation [9] and simplifying, we obtain a closed-form expression for the relative error of the approximation:

$$E(x) = \frac{\int_0^x p_a(\delta)\varepsilon_y(\delta)d\delta - \int_0^{d_{max}} p_a(\delta)\varepsilon_x(\delta)d\delta}{\int_0^{d_{max}} p_a(\delta)\varepsilon_x(\delta)d\delta}$$ [16]

The roots of E(x)=0, which are comprised of those combinations of x, $p_a(\delta)$, $\varepsilon_x(\delta)$ and $\varepsilon_y(\delta)$ that force the numerator of the right-hand side of Equation [16] to zero, delineate the conditions under which the approximation is exact. Equation [16] may be rewritten in different ways to help determine the roots of E(x)=0. One way is to split the second integral in the numerator into its [0,x] and [x,d_{max}] components and collect the terms having common limits of integration:

$$E(x) = \frac{\int_0^x p_a(\delta)\{\varepsilon_y(\delta)-\varepsilon_x(\delta)\}d\delta - \int_x^{d_{max}} p_a(\delta)\varepsilon_x(\delta)d\delta}{\int_0^{d_{max}} p_a(\delta)\varepsilon_x(\delta)d\delta}$$ [17]

Because all of the functions $p_a(\delta)$, $\varepsilon_x(\delta)$ and $\varepsilon_y(\delta)$ are strictly non-negative, one case in which the approximation is exact is if $\varepsilon_x(\delta)=\varepsilon_y(\delta)$ on [0,x] *and* $p_a(\delta)=0$ on [x,d_m]. Because y>x, it follows that $\varepsilon_y(x)$>0.5 by the definition of the cutpoint of the PM$_y$ sampler. Consequently, the physical interpretation of these circumstances is that the PM in the ambient air has no particles larger than x *and* either that (a) both samplers are ideal or (b) the samplers are identical (i. e., x=y). The first condition is reasonably plausible; for example, in a laboratory setting, we might choose to use a Total Suspended Particulate (TSP) sampler whose cutpoint is at 45μm to sample manufactured dust with a maximum particle AED of 15μm. However, either (a) or (b) must be true to drive E(x) to zero. Case (a) is, of course, physically implausible, and case (b) is trivial. Other means of re-writing the numerator of Equation [16] generate fundamentally equivalent arguments. From Equation [17], we can therefore conclude that E(x) can never be zero. By itself, that does not imply that the approximation is fundamentally flawed, only that it can never be exact. The errors E(x) are strictly non-negative.

We wrote a computer program in Mathcad Plus 6.0 (Mathsoft, 1995) to perform the computations in Equation [16] under a number of different scenarios of practical interest (see Table 1, compiled for x=2.5μm). As expected, the values of E(x) were nearly always negative and frequently exceeded 50%. Positive values of E(x) are attributable to errors associated with numerical integration and/or rounding under conditions in which the approximation is nearly exact.

When d_m>x, the logical extension of case (b) illuminates the fundamental weakness of the approximation. Consider the implications of the approximate method in the limit as x approaches y – that is, the limiting behavior of a PM$_x$ sampler as its performance characteristics approach those of the PM$_y$ sampler. This limiting behavior is shown graphically in Figure 5.

For an example scenario with a uniformly distributed ambient aerosol and non-ideal samplers, the cumulative particle-size distribution $P_{sy}(\delta)$ of the sampled particulate is a sigmoid with a mass median diameter (d_m) near the sampler cutpoint. (By definition, $P_{sy}(d_m)$=0.5.) The exact value of $P_{sy}(x)$ depends on the ambient PSD, but in our Mathcad simulations, $P_{sy}(x)$ was frequently between 0.4 and 0.7 in the limit as x approaches y. The approximate method stipulates that $C_{sx}=C_{sy}P_{sy}(x)$, which in the limit is approximately 0.5C_{sy}. C_{sy}, though, is the mass of PM$_y$ determined by gravimetry. The error is immediately obvious: in the limit as x approaches y, a PM$_x$ sampler should become indistinguishable from the PM$_y$ sampler, and C_{sx} should therefore approach C_{sy}. However, the approximate method implies that $C_{sx}=0.5C_{sy}$! The relative error in this limiting case is on the order of (-)30-60%, which is roughly equivalent to the errors computed using the Mathcad simulation.

The last point is perhaps difficult to see. Another way of looking at the logic error is to posit (a) the same PM$_y$ reference sampler and (b) a collocated PM$_{y+\Delta y}$ sampler, where Δy is a

differentially small increment in sampler cutpoint. All other operating parameters being equal, these two samplers will generate virtually the same C_s and $P_s(\delta)$. In the case of the reference sampler, (a), the mass of PM_y collected by the sampler is said to be C_s; in the case of sampler (b), however, the mass of PM_y collected by the sampler is kC_s, where k is a fraction approaching the value $P_{sy}(d_{cy})$ in the limit as Δy vanishes (see Figure 5). Again, the value of k will vary with the shape of $p(\delta)$, but only under narrowly controlled, laboratory conditions with nearly ideal samplers will k exhibit the correct limiting behavior for a valid approximate method, which would be 1.0.

Summary

Because of the relatively high cost of ambient monitoring for fine particles, and the variability associated with the cumbersome field protocols, some authors have proposed the use of particle-size distributions in conjunction with coarse-particle monitoring data to infer fine-particle concentrations in narrowly defined research conditions (Herber, 1988 and Buch et al., 1998). The logic of the proposed, approximate method is simple and straightforward and offers real promise in reducing the cost of ambient monitoring for non-volatile fine particles. However, our mathematical analysis shows that the approximate method gives erroneous results over a wide range of expected field conditions. The practical errors, as this analysis reveals, are actually systemic errors resulting from subtly flawed mathematical logic. In fact, the approximate method is only correct under narrowly drawn circumstances unlikely to occur in ambient monitoring applications. The approximate method is most accurate when the characteristic AED of the fine particles in question is very small in comparison to the cutpoint of the coarse-fraction sampler from which the fine-particle concentration is to be inferred (e. g., inferring non-volatile $PM_{2.5}$ concentrations from TSP measurements). In that case, the fractional penetration efficiency of the coarse-fraction sampler is nearly 100% for the corresponding fine particles. When the characteristic AED of the fine fraction under consideration is relatively close to the cutpoint of the coarse-fraction sampler, the errors of the approximation may exceed 70%. To improve its accuracy for compliance monitoring, the approximate method needs to account explicitly for the fractional penetration efficiency of the coarse-fraction sampler in its mathematical development.

References

Buch, U. M., C. B. Parnell, B. W. Shaw and B. W. Auvermann. 1998. Particle size results from the cascade impactor and the Federal Reference Method (FRM) $PM_{2.5}$ sampler using the Coulter Counter Multisizer. Presented at the Annual International Meeting of the American Society of Agricultural Engineers, Orlando, FL, July 12-16. Paper No. 98-4065.

Herber, D. J. 1988. Performance evaluation of PM_{10} and high-volume air samplers using a Coulter Counter particle size analyzer. Master of Science Thesis, Department of Agricultural Engineering, Texas A&M University, College Station, TX.

MathSoft, 1995. *Mathcad Plus 6.0 User's Guide.* Cambridge, MA: MathSoft, Inc. 694 pp.

USEPA. 1997a. Federal Reference Method for ambient sampling of coarse particulate matter (PM_{10}). 40 CFR Part 50 Appendix J.

USEPA. 1997b. Federal Reference Method for ambient sampling of fine particulate matter ($PM_{2.5}$). 40 CFR Part 50 Appendix L.
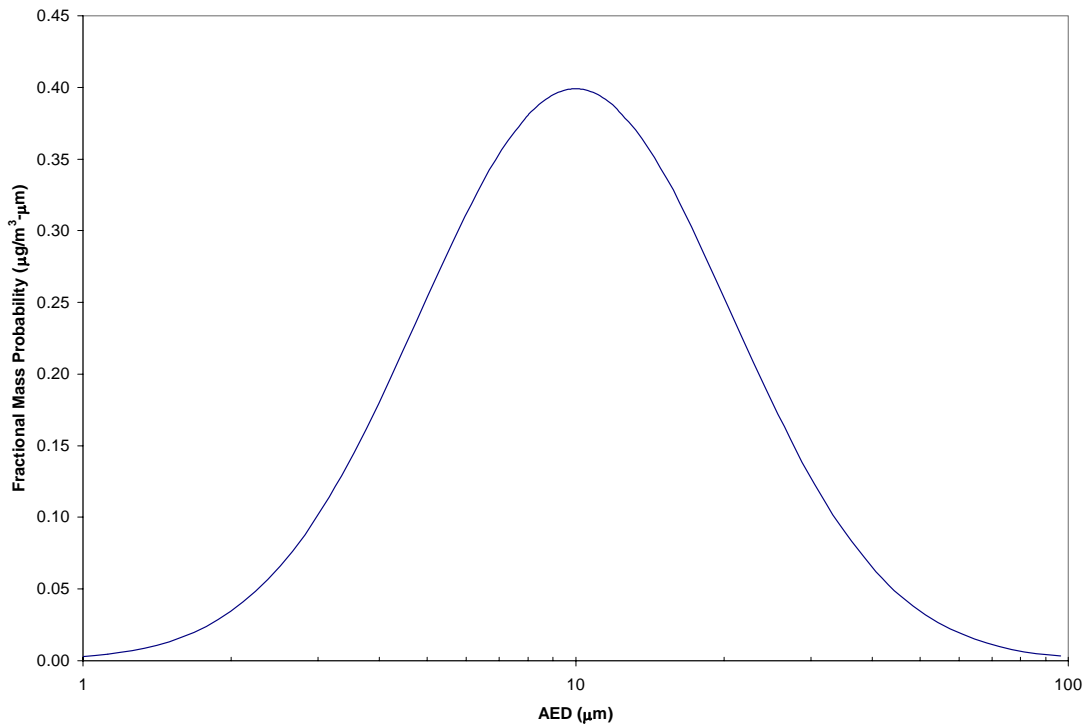
Figure 1.   Graphical representation of an idealized (log-normal) probability distribution relating particle mass to the aerodynamic equivalent diameter (AED) of the particles in the ensemble. By definition, the area under the curve is unity.
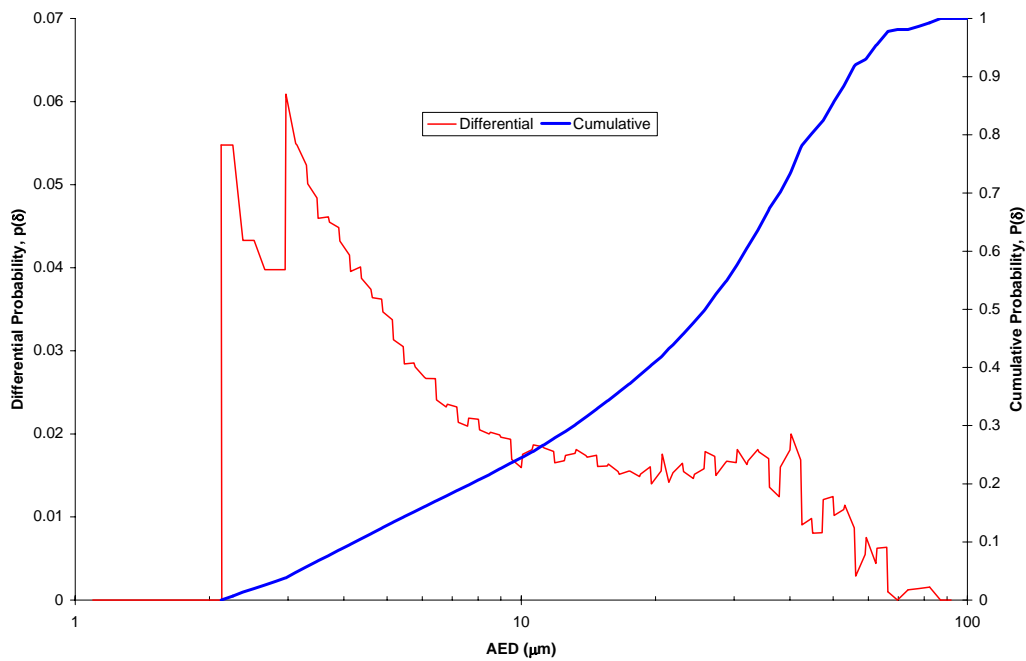

Figure 2.   Cumulative probability distribution $P_s(\delta)$ and differential probability distribution $p_s(\delta)$ for a sample of manufactured feedyard dust. Note that the maximum value of δ is 100µm, reflecting the fact that 100% of the sample mass is composed of particles having an AED less than or equal to 100µm. The distributions were determined using a Coulter Counter Multisizer (Herber, 1988).
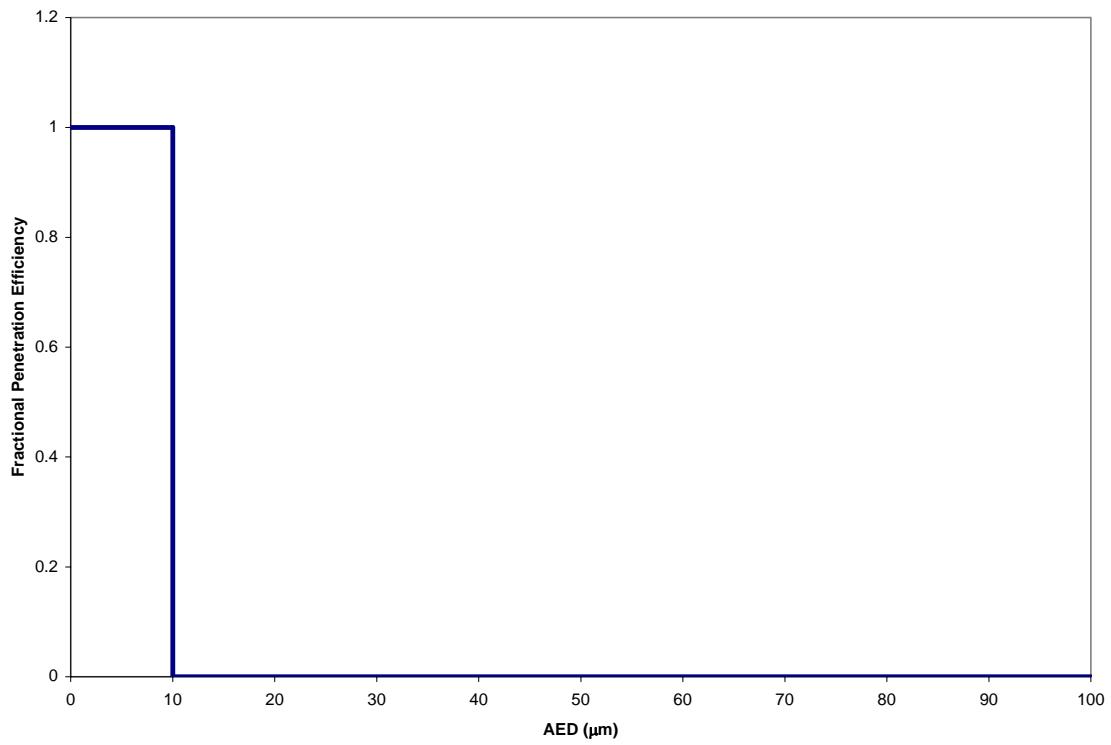
Figure 3.   Fractional penetration efficiency $\varepsilon(\delta)$ for an ideal sampler designed to sample particles having an AED less than or equal to 10μm.
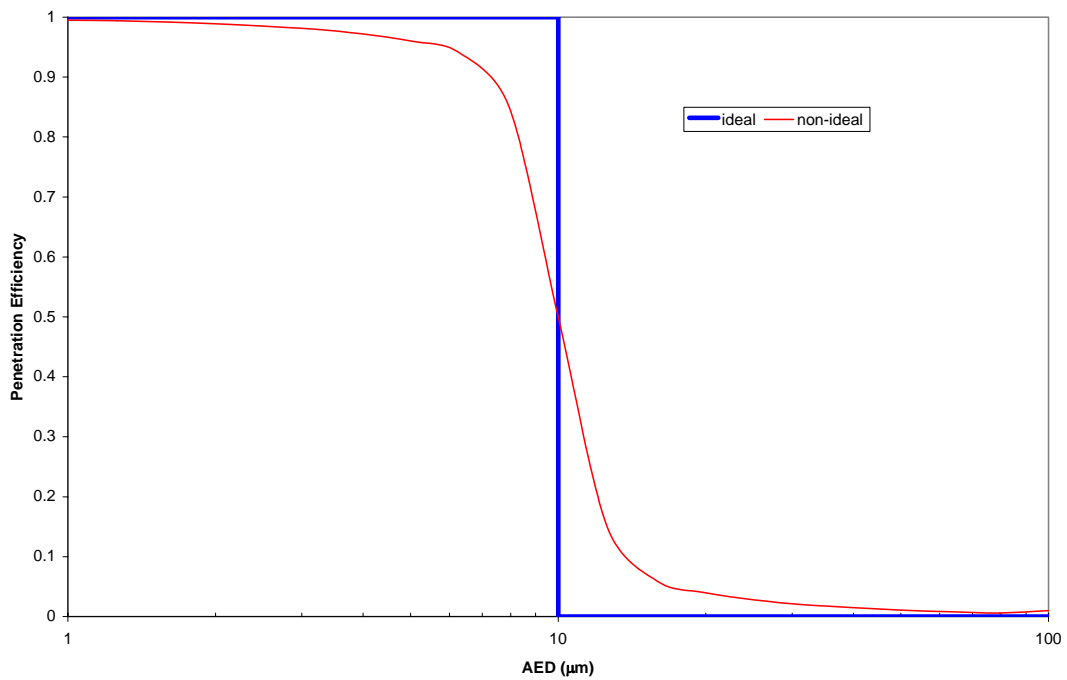

Figure 4.   Fractional penetration efficiency curves (a) for an ideal PM_{10} sampler and (b) for an actual (or non-ideal) PM_{10} sampler. In this case, "ideal" is defined in terms of a sampling objective to measure the total mass of PM having an AED less than or equal to 10μm. Note the logarithmic scale on the horizontal axis.

Table 1.   Summary of Test Scenarios and Associated Relative Errors E(x) Resulting from the Approximate Method.

| Run #	p(δ) Shape Class	d_{max} or d_{peak} (mm)	d_{cx} (mm)	d_{cy} (mm)	σ_g	$E(d_{cx})$ (%)	Comments
1	Uniform	d_{max}=5	2.5	10	1	-1.2	Ideal PM$_{10}$ samplers with d_{max}<<d_{cy} and uniform p(δ) on [0,5]
2	Uniform	d_{max}=25	2.5	10	1	-41.1	Ideal PM$_{10}$ samplers with d_{max}>d_{cy} and uniform p(δ) on [0,25]
3	Uniform	d_{max}=100	2.5	10	1	-76.7	Ideal PM$_{10}$ samplers with d_{max}>>d_{cy} and uniform p(δ) on [0,100]
4	Uniform	d_{max}=5	2.5	45	1	0.3	Ideal TSP samplers with d_{max}<<d_{cy} and uniform p(δ) on [0,5]
5	Uniform	d_{max}=25	2.5	45	1	-40.2	Ideal TSP samplers with d_{max}<d_{cy} and uniform p(δ) on [0,25]
6	Uniform	d_{max}=100	2.5	45	1	-76.2	Ideal TSP samplers with d_{max}>>d_{cy} and uniform p(δ) on [0,100]
7	Triangular	d_{peak}=5	2.5	10	1	-89.5	Ideal PM$_{10}$ samplers with d_{cx}<<d_{cy} and triangular p(δ)
8	Triangular	d_{peak}=5	9	10	1	-43.9	Ideal PM$_{10}$ samplers with d_{cx} close to d_{cy} and triangular p(δ)
9	Triangular	d_{peak}=5	2.5	45	1	-89.3	Ideal TSP samplers with d_{cx}<<d_{cy} and triangular p(δ)
10	Uniform	d_{max}=5	2.5	10	1.5	-9.7	Non-ideal PM$_{10}$ samplers with d_{max}<<d_{cy} and uniform p(δ) on [0,5]
11	Uniform	d_{max}=25	2.5	10	1.5	-44.5	Non-ideal PM$_{10}$ samplers with d_{max}>d_{cy} and uniform p(δ) on [0,25]
12	Uniform	d_{max}=100	2.5	10	1.5	-77.3	Non-ideal PM$_{10}$ samplers with d_{max}>>d_{cy} and uniform p(δ) on [0,100]
13	Uniform	d_{max}=5	2.5	45	1.5	-7.5	Non-ideal TSP samplers with d_{max}<<d_{cy} and uniform p(δ) on [0,5]
14	Uniform	d_{max}=25	2.5	45	1.5	-43.1	Non-ideal TSP samplers with d_{max}<d_{cy} and uniform p(δ) on [0,25]
15	Uniform	d_{max}=100	2.5	45	1.5	-76.7	Non-ideal TSP samplers with d_{max}>>d_{cy} and uniform p(δ) on [0,100]
16	Triangular	d_{peak}=5	2.5	10	1.5	-89.9	Non-ideal PM$_{10}$ samplers with d_{cx}<<d_{cy} and triangular p(δ)
17	Triangular	d_{peak}=5	9	10	1.5	-50.5	Non-ideal PM$_{10}$ samplers with d_{cx} close to d_{cy} and triangular p(δ)
18	Triangular	d_{peak}=5	2.5	45	1.5	-89.6	Non-ideal TSP samplers with d_{cx}<<d_{cy} and triangular p(δ)
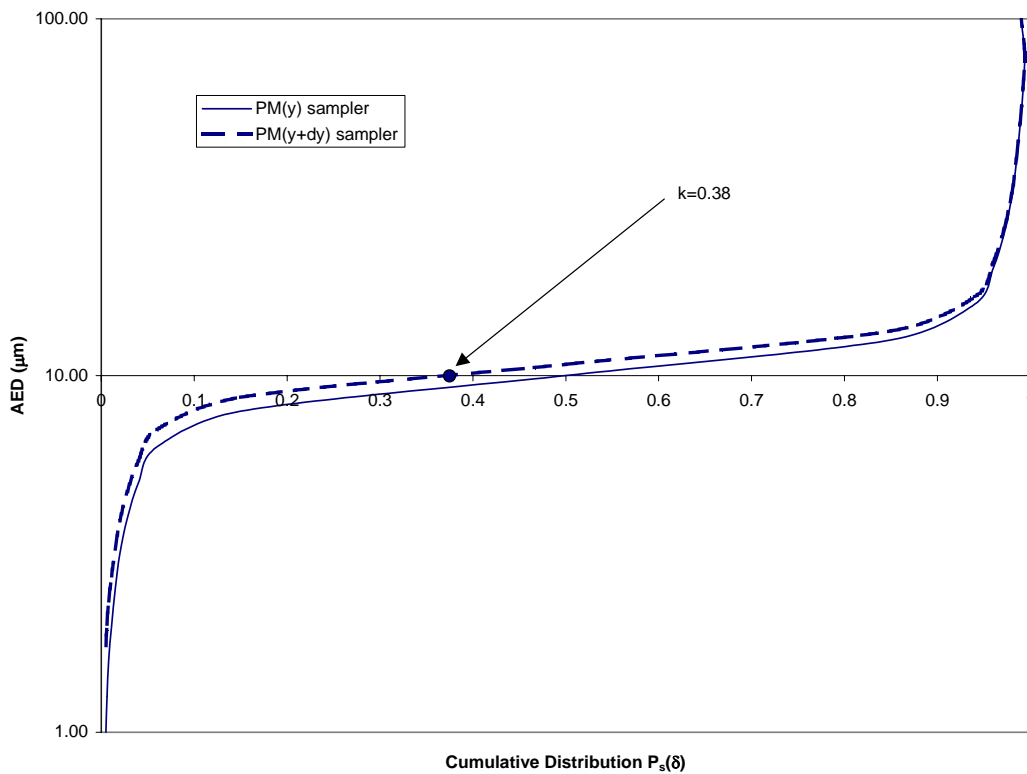
Figure 5.   Graphical illustration of the limiting behavior of the approximate method as the cutpoint of the fine-particle sampler approaches the cutpoint of the coarse-particle sampler. Note that the axes have been transposed from the traditional configuration for this plot of $P_s(\delta)$.